Journal of Renewable
Energy and Environment

Research Article

Journal Homepage: www.jree.ir

Frequency Control of Islanded Microgrids Based on Fuzzy Cooperative and Influence of STATCOM on Frequency of Microgrids

Maryam Rahmani[a], Faramarz Faghihi[a], Hassan Moradi CheshmehBeigi[b*], Seyed Mehdi Hosseini[c]

[a] *Department of Electrical and Computer Engineering, Faculty of Engineering, Islamic Azad University, Tehran, Iran.*
[b] *Department of Electrical Engineering, Razi University, Kermanshah, Iran.*
[c] *Department of Electrical Engineering, Babol Noshirvani University of Technology, Babol, Iran.*

PAPER INFO

Paper history:
Received 05 June 2019
Accepted in revised form 06 October 2019

Keywords:
Frequency Control
Fuzzy Logic
Static Synchronous Compensator
Microgrid

ABSTRACT

In this paper, the effect of a static synchronous compensator (STATCOM) influence on the frequency of islanded microgrids based on frequency control using fuzzy cooperative control is investigated. To achieve fast frequency control, instantaneous power balance between generation and consumption is inevitable, and it can be supplied through energy storage systems such as battery with a proper frequency control method. Besides, the frequency control of islanded microgrids could be studied under different circumstances, where one aspect analyzed is added to a flexible AC transmission system (FACTS) device, such as STATCOM, in the microgrids. Although STATCOM is charged with improving the voltage profile, it can affect frequency stability by adjusting the voltage very quickly. Due to the importance of refining frequency stability, two controller methods are compared: a classic PI controller and a fuzzy PID controller. Accordingly, the performance of STATCOM is evaluated via two scenarios. Based on simulation results, by applying the fuzzy PID controller to the microgrid, STATCOM can reach the nominal frequency. Moreover, with greater validation and investigation of this topic, this device could be an agreeable alternative to the battery energy storage system (BESS).

1. INTRODUCTION

Nowadays, power engineers have become highly enthusiastic to use renewable energy resources in the grids due to several reasons such as the high price of fossil fuels, non-renewability, and bioenvironmental aspect [1]. In particular, due to the effect of the political and economic situations in every country, fossil fuels price is increasing daily [2]. Due to these situations, there is an urgent need for governments to investigate renewable energies and microgrids [3]. Microgrid concept is defined while DGs are congregated in a distribution network [4]. Microgrid's power quality and service reliability control are two fundamental technical aspects during implementing a change [5]. Generally, a microgrid can work in connected and islanded modes [6]. The primary concern of the microgrid structure and its development is how to make it stronger against frequency fluctuations. For instance, in order to reduce frequency deviation and enhance the system robustness, the frequency control of the double sliding mode (SM) was designed for an islanded microgrid [7]. On the other hand, to improve the voltage profile of the grid, FACTS devices, such as Static Synchronous Compensator (STATCOM), could be implemented. Applying STATCOM, authors attempted to improve voltage profile, enhance the low voltage ride through (LVRT) capability, and provide a stronger grid against faults [8]. In some studies, power quality problems such as voltage fluctuation and voltage flicker that are critical for system performance in the presence of STATCOM were discussed [9,10]. In addition, it is vital for microgrids to maintain a voltage profile in order to boost their stability either in the grid-connected or islanded mode. The effect of STATCOM on microgrid's voltage profile in the grid-connected mode was investigated [10]. Another similar work on STATCOM in microgrids was performed [11], which focused on the profile voltage of two microgrids with a different controller for STATCOM. Among all of the control methods such as master-slave control, centralized control, and droop control [12,13], the cooperative control of microgrids provides an opportunity for DGs to make a strong connection with other components in which they could transfer information through a local network [14,15]. Typically, the best desired control performance should be able to make a strong connection between elements in the microgrid in order to gather data and have an extreme central controller to evaluate all data [16]. It is well documented that, in a PI controller, there are several defects such as parameter alternation vulnerability and system nonlinearity [17]; nonetheless, advantages of Fuzzy Logic Controllers (FLC) outweigh their disadvantages [18]. Features such as fast adaptability to nonlinear systems, non-required mathematical system, and better performance make the fuzzy controller the most dependable one [19]. In this study, fuzzy cooperative frequency control is compared to a classic controller (PI) in order to find the best desired controller. Accordingly, fuzzy cooperative frequency control is carried out as an appropriate control method. Moreover, to the best of the authors' knowledge, no results about the effectiveness of STATCOM on frequency stability and voltage profile improvement in an islanded microgrid have been found. The simulation process here is divided into two sections: the first section is dedicated to assessing the superiority of the fuzzy controller; the next section is presented to evaluate the effectiveness of

*Corresponding Author's Email: ha.moradi@razi.ac.ir (H. Moradi CheshmehBeigi)

STATCOM through two scenarios. The article is prearranged as follows: Section 2 deliberates the materials and methods of the paper. Section 3 expounds the control strategy of the microgrid. Section 4 itemizes results and discussion of simulation study; ultimately, Section 5 concludes the paper.

2. MICROGRID

As depicted in Fig. 1, the microgrid includes two diesel generators, one wind turbine system (WTS), a STATCOM, a BESS, and four loads. The characteristics of the system model are shown in Table 1 [20-22].

2.1. The wind turbine system

As shown in Fig. 2, the main components of a WTS include a wind turbine that converts wind energy into mechanical energy, a generator that is an implement for the conversion of mechanical energy into electrical energy, a rectifier, and an inverter [23].

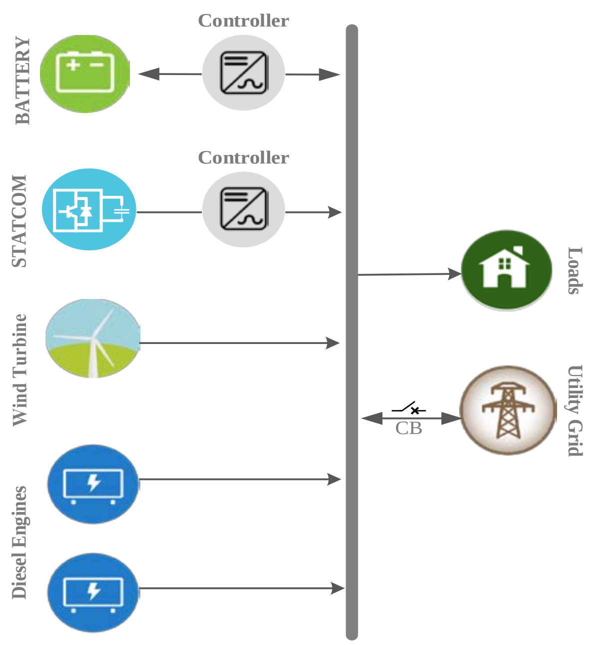

Figure 1. Schematic diragram of the studied microgrid.

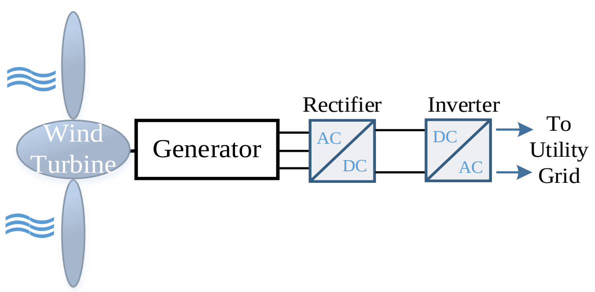

Figure 2. Wind turbine schematic diagram.

The mechanical power, P_m, hangs on four amounts: A_r as the area where the turbine blades sweep, V as the wind speed, ρ as the air density, and C_P as the rotor power coefficient and created by [24]:

$$P_m = 0.5.C_P(\lambda.\beta).\rho.A.V^3 \tag{1}$$

C_P signifies the percentage of the captured wind power converted by a wind turbine, and it is a function of pitch angle β and tip speed ratio (TSR) λ, which are defined as follows [25]:

$$C_P = 0.22(116\lambda_i - 0.4\beta - 5)e^{-125\lambda_i} \tag{2}$$

$$\lambda = \frac{\Omega R}{V} \tag{3}$$

where Ω is the rotor rotational speed, and R is the rotor radius of the wind turbine.

Table 1. System charactristics.

System parameters	Values
Diesel generator 1	18 KVA
Diesel generator 2	13 KVA
Wind turbine	25 KW
STATCOM	100 KW
BESS	56 KWh
Load 1	6 KW
Load 2	16+j3K
Load 3	15+j8k
Load 4	12+j8K

2.2. Diesel engine

Diesel engines play the main role in the cooperative frequency control; in fact, the output power factors of every microsource are determined. They collaborate with BESS to achieve power balance in the microgrid. P_i is defined by the power output of diesel engines, and P_{diss} is the dissipated power. The equation of energy conversion in diesel engine and power output can be printed as follows [24]:

$$P_i - P_{diss} = 0 \tag{4}$$

$$P_i = P_{ci}.n_i.m_f \tag{5}$$

where P_{ci} is the calorific value of the fuel, n_i is the indicated engine performance, and m_f is the flow of fuel injected into the combustion chamber. The dissipated power can be conveyed by [26]:

$$P_{diss} = P_{mf}.\frac{C_y}{4\pi}.\omega + C_r.\omega \tag{6}$$

where P_{mf} is the average pressure of the friction losses, C_y is the total displacement of the engine, C_r is the resistive torque to the applied load, and ω is the speed of the intake air of the engine.

2.3. Application of STATCOM in the microgrid

In this paper, as shown in Fig. 3., STATCOM comprises a coupling transformer, an inverter, and a DC capacitor along with a resistor. $U_{ed_{SC}}$ and $U_{eq_{SC}}$ are the initial inputs of a pulse width modulation method (PWM), responsible for determining the triggering angle of inverters and, eventually, controlling the STATCOM [27]. Thereby, the STATCOM active power potential is very low; nevertheless, its active power potential can be improved if an energy storage device is presented across the DC capacitor and the voltage is adjusted hastily. Hence, STATCOM in the microgrid is located in the nearest point to the BESS, as shown in Fig. 1. Fig. 4 shows the STATCOM system controller. As evidently demonstrated, the voltage and current of STATCOM (I_{sc}, V_{sc}) with the assistance of θ from phase-lock loop (PLL) block are converted to their $d-$ and $q-$ axis versions (I_{dsc}, I_{qsc}, V_{dsc}, and V_{qsc}).

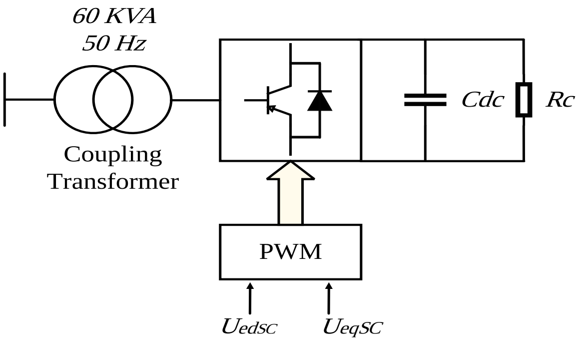

Figure 3. Wind turbine block diagram.

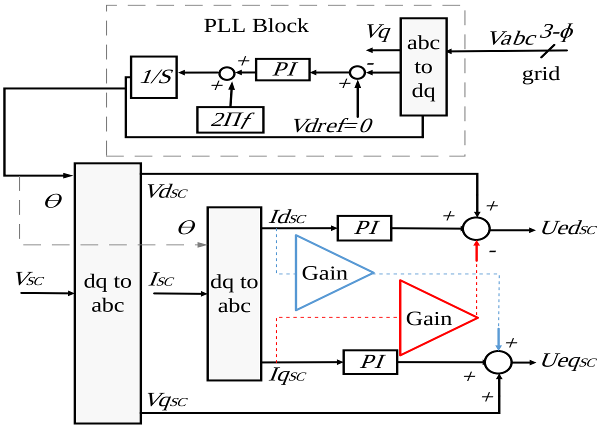

Figure 4. STATCOM controller block diagram.

Ultimately, in order to achieve U_{edsc} and U_{eqsc}, the PI controller with a trial-and-error method is applied [8, 9]. U_{edsc} and U_{eqsc} are given by:

$$U_{edsc} = V_{dsc} + K_i I_{dsc} + K_p \int I_{dsc}\, dt - \text{Gain} \times I_{qsc} \tag{7}$$

$$U_{eqsc} = V_{qsc} + K_i I_{qsc} + K_p \int I_{qsc}\, dt + \text{Gain} \times I_{dsc} \tag{8}$$

3. CONTROL STRATEGY

A management microgrid system (MMS) is a powerful control platform with a layered architecture. A local control (LC) is a controller placed on each component and checks the power output. A microgrid has two control layers: MMS and LC (see Fig. 5). The MMS manages the LC of each element in the microgrid. It causes BESS and diesel engines to determine a power output set point (POSP) and, then, LCs are presented with collected local information.

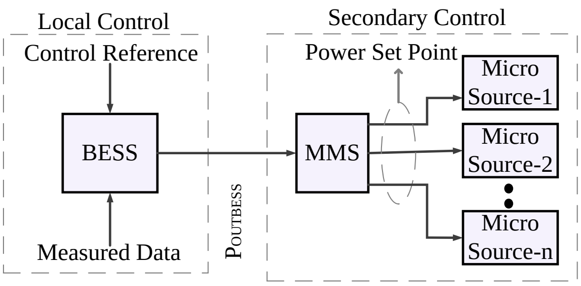

Figure 5. Layers of control strategy.

3.1. Local control

Fig. 6 shows all of the details of local control. It is well documented that when the microgrid enters islanding state, its control changes from PQ control state to vf control state, and this interaction occurs by all information collected by MMS. $I_{d_{ref}}$ and $I_{q_{ref}}$ are the current references, and I_d and I_q are the measured values. $V_{d_{ref}}$ and $V_{q_{ref}}$ (the voltage references) are yielded based on the difference between $I_{d_{ref}}$ and I_d, respectively (see (9) – (12)) [21].

$$I_1 = K_1(I_{d_{ref}} - I_d) + K_2 \int (I_{d_{ref}} - I_d) dt \tag{9}$$

$$I_2 = K_3(I_{q_{ref}} - I_q) + K_4 \int (I_{q_{ref}} - I_q) dt \tag{10}$$

$$V_{d_{ref}} = V_d + \omega L I_q - I_1 \tag{11}$$

$$V_{q_{ref}} = V_q - \omega L I_d - I_2 \tag{12}$$

where K_1, K_2, K_3, and K_4 are produced by the trial-and-error method. In consequence, with the application of the $d-q$ to abc block converter, the voltage references into an a-, b-, and c-axes, reference voltages ($V_{a_{ref}}$, $V_{b_{ref}}$, and $V_{c_{ref}}$) are created. A phase signal produced by the PLL block causes the PWM to perform. It controls the BESS by determining firing angles of an inverter. On the other hand, $I_{q_{ref}}$ (see (13)) is calculated, and K_5 and K_6 are formed by trial and error, as well.

$$I_{q_{ref}} = K_5(V_{ref} - V_{dc}) + K_6 \int (V_{ref} - V_{dc})\, dt \tag{13}$$

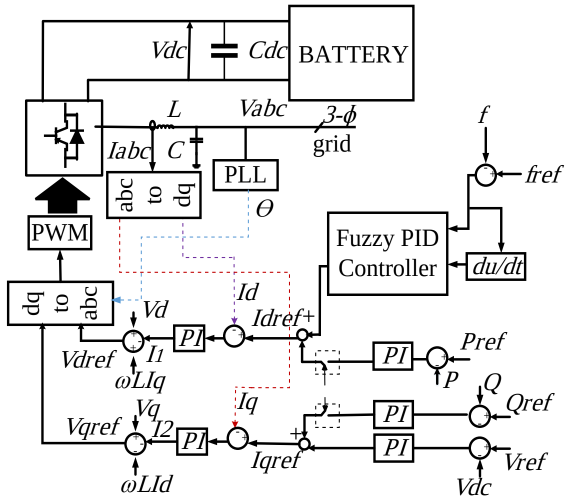

Figure 6. Local control of BESS.

Furthermore, in this study, two control methods are considered to evaluate their performance. When a PI controller is applied, $I_{d_{ref}}$ is achieved in the same manner as $I_{q_{ref}}$. On the other hand, when a fuzzy PID controller is presented, this current is created, as indicated in the following.

3.1.1. Fuzzy PID controller

As shown in Fig. 7, a fuzzy PID controller is applied in order to calculate $I_{d_{ref}}$. This controller has two inputs: error (ERROR) and derivative of error (ERROR*) (see (14), (15) [21].

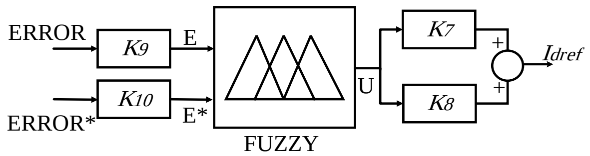

Figure 7. Configuration of the fuzzy PID controller.

$$e = \mathrm{ERROR} = f_{ref} - f \tag{14}$$

$$e^* = \mathrm{ERROR}^* = {}^{d}\!/_{dt}\,(f_{ref} - f) \tag{15}$$

The equations of $I_{d_{ref}}$ and U are:

$$I_{d_{ref}} = K_7 U + K_8 \int U dt \tag{16}$$

$$U = A + PE + DE^* \tag{17}$$

where

$$E = K_9 e \tag{18}$$

$$E^* = K_{10} e^* \tag{19}$$

Then $I_{d_{ref}}$ is:

$$I_{d_{ref}} = K_7 A + K_8 At + K_7 K_9 Pe + K_8 K_{10} De + K_8 K_9 P \int e dt + K_7 K_{10} De^* \tag{20}$$

After defining the controller gains (K_7, K_8, K_9, and K_{10}), membership functions and control rules become key techniques in designing the fuzzy PID controller. In general, the authors determined these functions and rules with their knowledge, experience, and the trial and error. Table 2 indicates that these membership functions have four memberships comprising five triangular memberships. The controller gains are defined by the PSO algorithm. More information can be found in [21].

Table 2. Fuzzy rules.

$P_{FLC(n)}$		ERROR*			
		N	Z	P	BP
ERROR	NB	N	BN	N	MN
	N	Z	Z	Z	N
	Z	Z	Z	Z	Z
	P	Z	Z	Z	P
	BP	P	BP	P	MP

3.2. Secondary control of MMS

Fig. 8 illustrates the secondary control layer of MMS. The total needed power (P_T and Q_T) produces POSP of microsources in order to return $P_{OUTBESS}$ to zero (see (21) and (22)) [20].

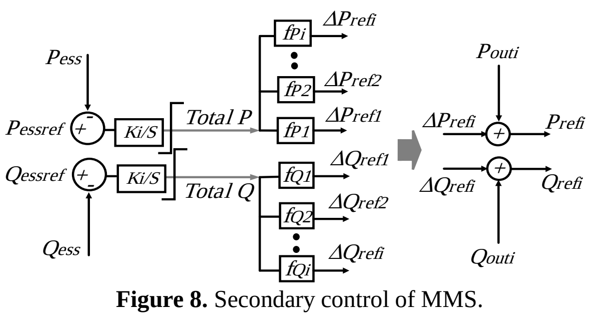

Figure 8. Secondary control of MMS.

$$\Delta P_{ref_i} = f_{Pi} \times P_T \tag{21}$$

$$\Delta Q_{refi} = f_{Qi} \times Q_T \tag{22}$$

where f_{Pi} and f_{Qi} are the factors evaluated by the capacity of each component such as a wind turbine in the microgrid.

$$f_{Pi} = \frac{P_{av_i}}{P_{T_{av}}},\ f_{Qi} = \frac{Q_{av_i}}{Q_{T_{av}}} \tag{23}$$

$$P_{T_{av}} = \sum_i^n P_{av_i},\ Q_{T_{av}} = \sum_i^n Q_{av_i} \tag{24}$$

where P_{av_i} and Q_{av_i} are the available active and reactive power of the ith DG unit. $P_{T_{av}}$ and $Q_{T_{av}}$ are the total available active and reactive power of the DG units in the microgrid. ΔP_{refi} and ΔQ_{refi} are the POSP alteration for the ith micro source. P_{OUTi} and Q_{OUTi} are the power outputs of thie th micro source at the moment. Eventualy, the refrence active power output of the ith microsource (P_{refi}) is produced by the summation of P_{OUTi} and ΔP_{refi}. Similarly, refrence Reactive power output (Q_{refi}) is generated in the same manner (see (25) and (26)).

$$P_{refi} = \Delta P_{refi} + P_{OUTi} \tag{25}$$

$$Q_{refi} = \Delta Q_{refi} + Q_{OUTi} \tag{26}$$

4. RESULTS AND DISCUSSION

Frequency control of the islanded microgrid is a common subject that has been presented in several cited papers such as [28-34]. In addition, the application of FACT devices, such as STATCOM, could help the microgrid improve its voltage profile. As a matter of fact, the analysis of the impact of STATCOM in the islanded microgrid is a new topic that could affect frequency due to a little active power injected to the system. In this paper, through a simulation study, due to the importance of achieving better results, two controller methods are compared: PI controller and Fuzzy PID controller. The frequency control model is implemented in MATLAB/SIMULINK software, and it is assumed that wind turbine and diesel generators thoroughly generate all of the command power of microgrid loads.

4.1. Finding a better controller

The simulation is obtained for two different controller methods without the presence of STATCOM. The first controller is a classic PI controller whose gains are obtained by trial and error. The second controller is a fuzzy cooperative controller that has been explained entirely, before. In both cases, after t=1 sec, the microgrid is working in the islanded mode. Fig. 9 shows the frequency diagram of the microgrid including these two cases. After islanding at t=1 sec, in each case, frequency stability is achieved quickly and, around t=1.02 sec, frequency is returned to the nominal frequency amount. Therefore, it is confirmed that these two methods are able to control the frequency precisely. The better control method is that which diminishes the frequency less than the other one.

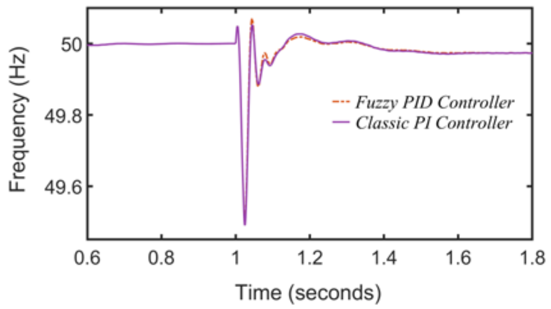

Figure 9. Frequency of two different control methods: PI and fuzzy PID controllers.

Fig. 10 shows the exact amount of the frequency of each controller. In the case that a classic controller is applied to the microgrid, the frequency is reduced to f_1=49.49 Hz. On the one hand, the fuzzy PID controller effectively contracts the amount of frequency to around f_2=49.499 Hz. The difference between f_1 and f_2 is around 0.01 Hz. It is crystal clear that the fuzzy PID method controls the frequency of the islanded microgrids better than the PI controller. Consequently, it can be noted that frequency control is improved by applying the fuzzy PID controller. As mentioned in Section 1, through the application of the fuzzy PID controller, frequency control is enhanced. Hence, in the next section, the fuzzy PID controller is applied to the microgrid. Section 2 contains two scenarios, which will analyze the effectiveness of STATCOM on the frequency control of the microgrid. Furthermore, in [35], the secondary control scheme through several scenarios was engaged to share the power disparity and control the frequency and voltage of the microgrid. In the two scenarios, similar to this paper, the controller reinstates the microgrid voltage and frequency to its nominal amount. In this paper, at t<0.2 s, frequency is returned to its normal value in every scenario; however, when the secondary control scheme is used, it takes about 1 second to regulate the frequency.

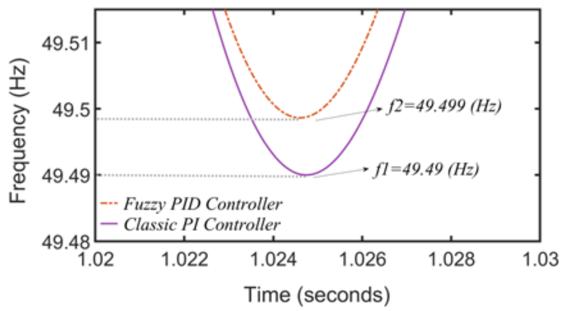

Figure 10. More detailed frequency comparison between the two controller methods.

4.2. STACOM effectiveness

4.2.1. First scenario

To ensure the effectiveness of STATCOM in the proposed cooperative frequency control, this scenario is considered. The microgrid is disconnected from the upper grid at t=1 sec. According to Fig. 11, frequency increases and reaches 58 Hz at t=1 sec. Regarding the rapid response of the BESS, frequency is returned to the normal boundary, which is between 49.7 Hz and 50.3 Hz only after 0.2 sec. In this situation, BESS injects power in order to provide a balance between loads and powers.

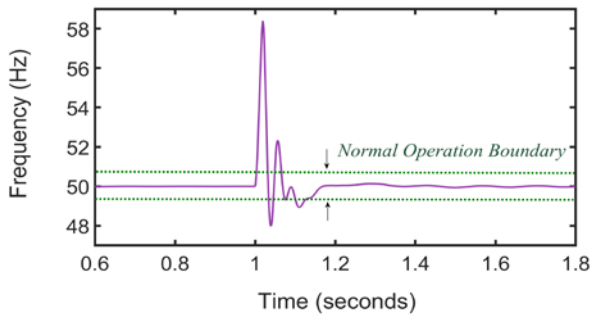

Figure 11. Frequency diagram of the microgorid in the first scenario.

As shown in Fig. 12, before t=0.6 sec, there is a voltage flicker that appears because of the application of STATCOM. The nominal voltage of the microgrid is 225 V. At t=1 sec, when the state of the microgrid changes to the islanded state, the voltage increases to 270 V in less than 0.01 sec, as shown in Fig. 12. After almost 0.2 sec, voltage arrives at its normal operation boundary. As indicated in Fig. 12, this boundary is about 210 V to 230 V. As a result, the STATCOM has a positive effect on voltage and frequency profile. In order to analyze the positive impact of STATCOM, the next scenario is proposed.

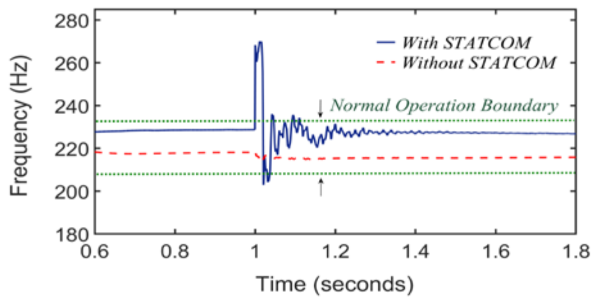

Figure 12. Voltage diagram of the microgrid–First scenario.

4.2.2. Second scenario

This scenario is designed for the case in which BESS is discharged after hours of working as an energy storage system in order to control the frequency of the islanded microgrid. During the next time of working in the grid-connected mode, at t=1 sec, the microgrid is disconnected from the grid, again. Simulation is done in two specific cases: Case 1: without STATCOM and BESS; Case 2: with the presence of STATCOM and without BESS. As shown in Fig. 13, in Case 1, without both of them, the frequency is lost. Hence, the balance between power supply and demand is mislaid. As a matter of fact, frequency stabilization is not achieved, because there is no component to aid the microgrid in order to respond to the alternations and maintain its stability.

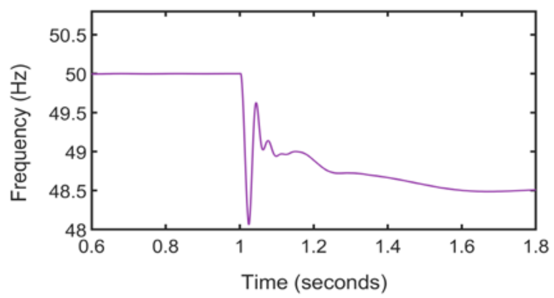

Figure 13. Frequency diagram of the microgrid–Second scenario/Case 1.

On the other hand, in Case 2, as shown in Fig. 14, frequency stabilization in the presence of STATCOM is concluded rapidly. It is well documented that, for the state that STATCOM is present around t=1.3 sec, frequency is returned to nominal frequency amount, which is 50 Hz, meaning that STATCOM could provide the power demand for the microgrid in order to stabilize frequency. As mentioned before, STATCOM could have an effect on frequency stabilization by adjusting the voltage very quickly.

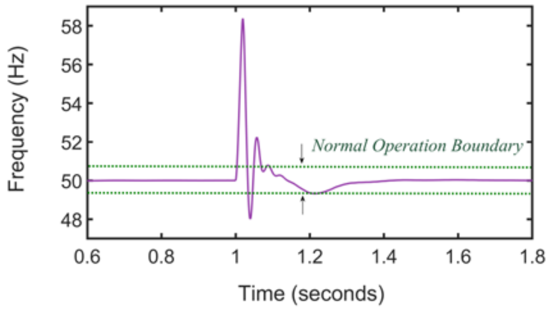

Figure 14. Frequency diagram of the microgrid–Second scenario/Case 2.

Fig. 15 shows that the improvement of voltage profile due to an increase in the reactive power of STATCOM. Thereby, voltage performs in its nominal amount. Voltage stabilization takes place at t=1.4 sec, 0.4 sec after being disconnected from the main grid. It is enough for the STATCOM to have an effect on the frequency amount.

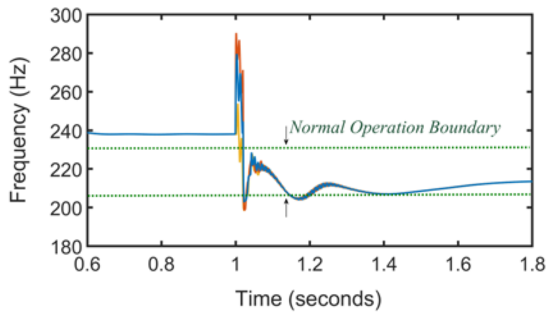

Figure 15. Voltage diagram of the microgrid-Second scenario/Case 2.

Fig. 16 suggests the reactive power of STATCOM in the second scenario in the presence of STATCOM. It is crystal clear that when the microgrid starts to work in the islanded mode, the power reactive will change.

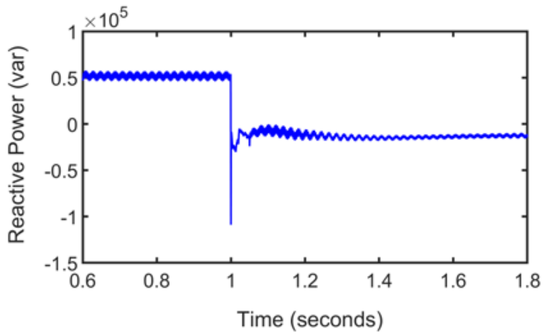

Figure 16. Reactive power of STATCOM in the Second scenario.

5. CONCLUSIONS

This paper analyzed the impact of STATCOM on the frequency of the islanded microgrid based on fuzzy cooperative frequency control. To improve its frequency, two control methods were investigated: a classic PI Controller and a Fuzzy PID Control method. Eventually, to evaluate the impact of STATCOM on selected cooperative frequency, control conditions with or without STATCOM were studied. In this study, two scenarios were presented. The STATCOM was assumed to be implemented at nearby BESS to evaluate its impact. With a comparison between the first and second scenarios, it could be concluded that, without BESS and STATCOM, there is no chance to control the frequency of the microgrid; on the contrary, in the presence of STATCOM with the lack of BESS, the frequency control is expected to occur. As a matter of fact, STATCOM cannot be used in the microgrids and, thus, acts as a frequency controller device solely, because not only does it force the system to encounter a wide range of frequency variations, but also its control system is designed for other achievements such as the improvement of the voltage profile. However, in certain situations such as discharging of the BESS, STATCOM could be of proper assistance in maintaining system stability. Finally, it could be a good recommendation for researchers to create a new device that plays the role of a STATCOM and BESS simultaneously so that the cost of application and maintenance of those two devices can decrease.

6. ACKNOWLEDGEMENT

The authors wish to thank the Islamic Azad University of Tehran, Science and Research Branch and the Razi University.

REFERENCES

1. Gargari, M.H., Sadrameli, S.M. and Taherkhani, M., "Investigating the batch and continuous transesterification of linseed oil by using a alkaline heterogeneous catalyst in a packed bed reactor", ***Journal of Renewable Energy and Environment (JREE)***, Vol. 4, No. 2&3, (2017), 1-9.
2. Tahani, M., Servati, P., Hajinezhad, A., Noorollahi, Y. and Ziaee, E., "Assessment of wind energy use to store the water for generation power with two stage optimization method", ***Journal of Renewable Energy and Environment (JREE)***, Vol. 2, No. 2, (2015), 23-28.
3. Golshannavaz, S. and Nazarpour, D., "Multi attribute investment planning of a grid-connected diesel/wind/PV/battery hybrid energy system", ***Journal of Renewable Energy and Environment (JREE)***, Vol. 1, No. 1, (2014), 43-52.
4. He, J., Li, Y. and Blaabjerg, F., "An enhanced islanding microgrid reactive power, imbalance power, and harmonic power sharing scheme", ***IEEE Transaction on Power Electronics***, Vol. 30, No. 6, (2014), 3389-3401. (DOI: 10.1109/TPEL.2014.2332998).
5. Zheng, F., Deng, C., Chen, L., Li, S., Liu, Y. and Liao, Y., "Transient performance improvement of microgrid by a resistive superconducting fault current limiter", ***IEEE Transaction on Applied Superconductivity***, Vol. 23, No. 3, (2015), 1-5. (DOI: 10.1109/ TASC.2015.2391120).
6. Liu, K., He, J., Luo, Z., Shen, X., Liu, X. and Lu, T., "Secondary frequency control of isolated microgrid based on LADRC", ***IEEE Access***, Vol. 7, (2019), 53454-53462. (DOI: 10.1109/ACCESS. 2019.2911911).
7. Wang, C., Mi, Y., Fu, Y. and Wang, P., "Frequency control of an isolated micro-grid using double sliding mode controllers and disturbance observer", ***IEEE Transactions on Smart Grid***, Vol. 9, No. 2, (2018), 923-930. (DOI: 10.1109/TSG.2016.2571439).
8. Mosaad, M., "Model reference adaptive control of STATCOM for grid integration of wind energy systems", ***IET Electric Power Applications***, Vol. 12, No. 5, (2018), 605-613. (DOI: 10.1049/iet-epa.2017.0662).
9. Pal, K., Panigrahi, B.K., Mohapatra, S. and Mohapatra, A., "Impact of STATCOM on voltage profile in a DG penetrated grid connected system", ***Proceedings of 2017 International Conference on Circuit,***

Power and Computing Technologies (ICCPCT), India, (2017). (DOI: 10.1049/iet-epa.2017.0662).

10. Hossain, E., Tür, M.R., Padmanaban, S., Ay, S. and Khan, I., "Analysis and mitigation of power quality issues in distributed generation systems using custom power devices", ***IEEE Access***, Vol. 6, (2018), 16816-16833. (DOI: 10.1109/ACCESS.2018.2814981).

11. Mohanty, K.B. and Pati, S., "Voltage profile improvement of micro-grids using SMC based STATCOM", ***Proceedings of 2016 Annual IEEE Systems Conference (SysCon)***, USA, (2016). (DOI: 10.1109/SYSCON.2016.7490609).

12. Hosen, M.S., Abir, M.Z.I., Rana, M.S. and Ali, M.M., "An optimal control of three phase islanded microgrid system", ***Proceedings of International Conference on Electrical, Computer and Communication Engineering (ECCE)***, Bangladesh, (2019). (DOI: 10.1109/ECACE.2019.8679112).

13. Huang, X., Wang, K., Qiu, J., Hang, L., Li, G. and Wang, X., "Decentralized control of multi-parallel grid-forming DGs in islanded microgrids for enhanced transient performance", ***IEEE Access***, Vol. 7, (2019), 17958-17968. (DOI: 10.1109/ACCESS.2019.2896594).

14. Romphochai, S. and Hongesombut, K., "Fuzzy logic voltage regulator for improving transient stability and fault ride through capability of DFIG wind turbines", ***International Review of Electrical Engineering (IREE)***, Vol. 10, No. 5, (2015), 670-677. (DOI: 10.670.10.15866/iree.v10i5.7403).

15. Lee, H.-S., Koo, B.-G., Lee, S.-W., Kim, W. and Park, J.-H., "Optimal control of BESS in microgrid for islanded operation using fuzzy logic", ***Proceedings of 5^th^ International Conference on Intelligent Systems, Modelling and Simulation***, Malaysia, (2014). (DOI: 10.1109/ ISMS.2014.86).

16. Lopes, J., Moreira, C. and Madureira, A., "Defining control strategies for microgrids islanded operation", ***IEEE Transaction on Power System***, Vol. 21, No. 2, (2006), 916-924. (DOI: 10.1109/TPWRS. 2006.873018).

17. Lai, J., Zhou, H., Lu, X., Yu, X. and Hu, W., "Droop-based distributed cooperative control for microgrids with time-varying delays", ***IEEE Transaction on Smart Grid***, Vol. 7, No. 4, (2016), 1775-1789. (DOI: 10.1109/TSG.2016.2557813).

18. Xu, Y., Zhang, W., Hug, G., Kar, S. and Lim, Z., "Cooperative control of distributed energy storage systems in a microgrid", ***IEEE Transactions on Smart Grid***, Vol. 6, No. 1, (2015), 238-248. (DOI: 10.1109/ TSG.2014.2354033).

19. Brearley, B.J. and Prabu, R.R., "A review on issues and approaches for microgrid protection", ***Renewable and Sustainable Energy Reviews***, Vol. 67, (2017), 988-997. (DOI: 10.1016/j.rser.2016.09.047).

20. Khan, Sh. and Bhowmick, S., "A novel power flow model of a static synchronous series compensator (SSSC)", ***Proceedings of 6^th^ IEEE Power India International Conference (PIICON)***, India, (2014). (DOI: 10.1109/POWERI.2014.7117606).

21. Kim, J.-Y., Kim, H.-M., Kim, S.-K., Jeon, J.-H. and Choi, H.-K., "Designing an energy storage system fuzzy PID controller for microgrid islanded operation", ***Energies***, Vol. 4, No. 9, (2011), 1443-1460. (DOI: 10.3390/en4091443).

22. Kim, J.-Y., Jeon, J.-H., Kim, S.-K., Cho, C.,Park, J.H., Kim, H.-M. and Nam, K.-Y., "Cooperative control strategy of energy storagesystem and microsources for stabilizing the microgrid during islanded operation", ***IEEE Transaction on Power Electronics***, Vol. 25, No. 12, (2010), 3037-3048. (DOI: 10.1109/TPEL.2010.2073488).

23. Mohammed, H. and Nwankpa, C.O., "Stochastic analysis and simulation of grid-connected wind energy conversion system", ***IEEE Transactions on Energy Conversion***, Vol. 15, No. 1, (2000), 85-90. (DOI: 10.1109/60.849121).

24. Toufouti, R., "Modeling and simulation of hybrid wind-diesel power generation system", ***International Journal of Renewable Energy***, Vol. 8, No. 2, (2013), 49-58. (DOI: 10.14456/iire.2013.11).

25. Allali, K., Azzag, E.B. and Kahoul, N., "Modeling and simulation of a wind-diesel hybrid power system for isolated areas", ***International Journal of Computer Applications***, Vol. 116, No. 23, (2015), 18-23. (DOI: 10.5120/20499-2409).

26. Jurado, F. and Saenz, J.R., "Neuro-fuzzy control autonomous wind-diesel systems using biomass", ***Renwable Energy Journal***, Vol. 27, No. 1, (2002), 39-56. (DOI: 10.1016/S0960-1481(01)00170-7).

27. Khan, S. and Bhowmick, S., "STATCOM modeling for power flow analysis", ***Proceedings of 6^th^ IEEE Power India International Conference (PIICON)***, India, (2014). (DOI: 10.1109/POWERI. 2014.7117603).

28. Arani, A.A.K., Gharepetian, G.B. and Abedi, M., "A novel control method based on droop for cooperation of flywheel and battery energy storage systems in islanded microgrids", ***IEEE Systems Journal***, (2019), 1-8. (DOI: 10.1109/JSYST.2019.2911160).

29. Mehmood, K.K., Khan, S.U., Lee, S.-J., Haider, Z.M., Rafique, M.K. and Kim, C.-H., "Optimal sizing and allocation of battery energy storage systems with wind and solar power DGs in a distribution network for voltage regulation considering the lifespan of batteries", ***IET Renewable Power Generation***, Vol. 11, No. 10, (2017), 1305-1315. (DOI: 10.1049/iet-rpg.2016.0938).

30. Ali, H., Magdy, G., Li, B., Shabib, G., Elbaset, A.A., Xu, D. and Mitani, Y., "A new frequency control strategy in an islanded microgrid using virtual inertia control-based coefficient diagram method", ***IEEE Access***, Vol. 7, (2019), 16979-16990. (DOI: 10.1109/ACCESS. 2019.2894840).

31. Ameli, H., Abbasi, E., Ameli, M.T. and Strbac, G., "A fuzzy-logic-based control methodology for secure operation of a microgrid in interconnected and isolated modes", ***International Transactions on Electrical Energy Systems***, Vol. 27, No. 11, (2017), 841-848. (DOI: 10.1002/etep.2389).

32. Lei, Q., Si, Y. and Liu, Y., "Energy storage system control strategy to minimize the voltage and frequency fluctuation in the microgird", ***Proceedings of 2018 IEEE Applied Power Electronics Conference and Exposition (APEC)***, USA, (2018). (DOI: 10.1109/APEC. 2018.8341215).

33. Issa, W.R., El Khateb, A.H., Abusara, M.A. and MallicK, T.K., "Control strategy for uninterrupted microgrid mode transfer during unintentional islanding scenarios", ***IEEE Transaction on Industrial Electronics***, Vol. 65, No. 6, (2018), 4831-4839. (DOI: 10.1109/ TIE.2017.2772199).

34. Awal, M.A., Yu, H., Tu, H., Lukic, S. and Husain, I., "Hierarchical control for virtual oscillator based grid-connected and islanded microgrids", ***IEEE Transactions on Power Electronics***, (2019), 1-14. (DOI: 10.1109/TPEL.2019.2912152).

35. Shotorbani, A., Ghassem Zadeh, S., Mohammadi-Ivatloo, B. and Hosseini, S.H., "A distributed secondary scheme with terminal sliding mode controller for energy storages in an islanded microgrid", ***International Journal of Electrical Power & Energy Systems***, No. 93, (2017), 352-364. (DOI: 10.1016/j.ijepes.2017.06.013).